



UNIVERSITY OF LEEDS

This is a repository copy of *The composition of tribofilms produced on metal-on-metal hip bearings*.

White Rose Research Online URL for this paper:
<https://eprints.whiterose.ac.uk/101416/>

Version: Accepted Version

Article:

Hesketh, J, Ward, M, Dowson, D orcid.org/0000-0001-5043-5684 et al. (1 more author)
(2014) The composition of tribofilms produced on metal-on-metal hip bearings.
Biomaterials, 35 (7). pp. 2113-2119. ISSN 0142-9612

<https://doi.org/10.1016/j.biomaterials.2013.11.065>

© 2013 Elsevier Ltd. All rights reserved. This is an author produced version of a paper published in Biomaterials. Uploaded in accordance with the publisher's self-archiving policy. This version licensed under the Creative Commons Attribution-NonCommercial-NoDerivatives 4.0 International (<http://creativecommons.org/licenses/by-nc-nd/4.0/>).

Reuse

Items deposited in White Rose Research Online are protected by copyright, with all rights reserved unless indicated otherwise. They may be downloaded and/or printed for private study, or other acts as permitted by national copyright laws. The publisher or other rights holders may allow further reproduction and re-use of the full text version. This is indicated by the licence information on the White Rose Research Online record for the item.

Takedown

If you consider content in White Rose Research Online to be in breach of UK law, please notify us by emailing eprints@whiterose.ac.uk including the URL of the record and the reason for the withdrawal request.



eprints@whiterose.ac.uk
<https://eprints.whiterose.ac.uk/>

The composition of tribofilms produced on metal-on-metal hip bearings

James Hesketh^{a, *}, Michael Ward^b, Duncan Dowson^a, Anne Neville^a

^aInstitute of Engineering Thermofluids Surfaces and Interfaces, Department of Mechanical Engineering, University of Leeds, Leeds, United Kingdom

^bLeeds Electron Microscopy and Spectroscopy Centre, School of Process Environmental and Materials Engineering, University of Leeds, Leeds, United Kingdom

Abstract

Following wear testing in a hip simulator, the bearing surfaces of 36 mm metal on metal total hip replacements showed the formation of tribochemical layers. These layers were investigated in a transmission electron microscope, and analysis was performed using electron energy loss spectroscopy, energy dispersive x-rays and selected area electron diffraction. The tribofilm formed at the edge of the wear scar was 100 s of nanometres thick and contained cobalt sulphide particles embedded within. The film itself was rich in carbon, and appeared to contain no long range graphitic ordering when analysed with electron energy loss spectroscopy, and the spectra gathered from the tribofilm closely resembled those collected from amorphous carbon. The location at which the most substantial tribological layers formed may be explained by the formation of a blunt wedge at the edge of the wear scar following conformal changes to the bearing surfaces.

Keywords

Tribology; Hip replacement; Transmission electron microscopy; Graphitisation

1. Introduction

Total joint replacement is the most successful treatment for end stage arthritis, and was used to restore functionality to over 85,000 people in the UK over 2011/12 [1]. One of the main challenges facing both engineers and surgeons in this field is to design and implant a joint replacement that can last the extent of a patient's life without need for revision. In 2011/12, approximately 10,000 hip replacements performed in the UK were revision surgeries, a figure that has been steadily rising since 2003.

One of the major factors leading to revision surgery is the biological response to the wear and corrosion debris produced by a joint replacement over its operational lifetime. A major source of this debris arises from the articulating bearing surfaces. Traditionally, metal-on-polymer [MoP] bearings have been the most popular material selection, however, due to their propensity to produce a large volume of bio-reactive polymeric wear particles, other material combinations have gained notoriety. One such combination is the metal-on-metal [MoM] bearing, usually consisting of cobalt-chromium [CoCr] alloys. MoM bearings produce a considerably lower volume of debris than MoP bearings, giving them the potential to outlast the 15 year lifetime usually experienced by MoP designs [2,3].

Despite enjoying a superior wear performance over MoP designs, it has come to light that MoM bearings suffer from a unique set of shortcomings. The particles produced by MoM bearings are of the order of tens of nanometres in size, which results in the formation of a considerable number of particles from a comparatively small loss in total volume [4-7]. The particles have been found to disseminate around the body, and have been linked to adverse soft tissue reactions in patients [8]. In addition, it has been found that CoCr alloys are susceptible to in vivo corrosion, leading to the production of cytotoxic metal ions, particularly Co^{2+} and Cr^{3+} [9-11].

Amidst these concerns, a large number of MoM implants function extremely well. Findings by Wimmer et al [12,13], suggest that this may be explained, in part, by the ability of MoM joint surfaces to form protective organometallic films on their surfaces. These films are termed tribochemical reaction layers [sometimes referred to as tribolayers or tribofilms]. Tribolayers were identified on a large number of explanted prostheses, as well as surfaces worn artificially in hip simulators. It has been shown that these layers are rich in organic carbon, originating from the joint fluid, in addition to metal oxides and a number of organic elements and salts. It was further demonstrated that the formation of these layers was the result of chemical changes being driven through the actions of mechanical mixing between the surface and upper subsurface.

Other authors have also reported the formation of organometallic layers forming during the wear and corrosion of CoCr alloys [14,15].

Recent findings suggest that graphitisation can take place within the carbon rich tribochemical reaction layers found on MoM bearing surfaces [16]. Electron energy loss spectroscopy of the carbon K- ionisation edge, and Raman spectroscopy were performed on samples of the reaction layer. Both suggested that the level of sp^2 bonding within the carbon was around 80%. In addition, high-resolution electron transmission microscopy [HRTEM] showed that the layer contained short range ordering with an electron diffraction fringe spacing of ~ 0.34 nm. Despite these findings, the mechanism by which graphitisation could occur under the modest pressures and temperatures experienced during the normal function of MoM hip replacements is still uncertain.

In this study, a detailed investigation of the structure and chemical properties of tribolayers formed during simulator testing is undertaken. As well as discussion of the mechanisms, which may contribute to their formation. Particular attention is given to the morphology and composition of particles embedded within the layer, to give a more complete understanding of the degradation of MoM joint replacements.

2. Methodology

Two 36 mm wrought, high-carbon, metal-on-metal hip bearings were tested in a single station Prosim 'deep flexion' hip simulator, with cups angled at a 45° inclination. Tests were run for 2/3 million cycles to approximate 8 months of in vivo activity. The gait cycle imposed was based on a Paul-type cycle with a peak load of

3 kN and a swing phase load of 50 N. Tests were lubricated with 25% v/v bovine serum solution, supplemented with 0.03% sodium azide to retard bacterial growth.

At 1/3 million cycles the test was stopped and the serum replaced, at which point the bearing surfaces were rinsed with distilled water and reassembled. Following 2/3 million cycles of testing, samples were rinsed with distilled water and placed in a desiccator.

Focused ion beam [FIB] transmission electron microscope [TEM] sections were prepared from the femoral heads using an FEI Nova 200 Nanolab dual beam scanning electron microscope [SEM]/FIB, fitted with a Kleindiek micromanipulator. The ion column was operated at 30 kV and 5 kV and at beam currents between 5 nA and 0.05 nA, and the electron column at 5 kV and 29 pA. The surface was initially covered in a 40 nm gold spluttered coating. The site of interest was then protected with a 200 nm electron deposited platinum layer, and then a 1-micron thick platinum layer deposited using the gallium ion beam. Surrounding material was then removed using the ion beam, and a section from the site of interest was removed using the micromanipulator and attached to a TEM support grid. The section was then thinned to <100 nm. TEM imaging, selected area electron diffraction [SAED] and energy dispersive X-ray [EDX] mapping was carried out using a FEI Tecnai F20 FEGTEM operated at 200 keV and fitted with a Gatan SC600 CCD camera and a high angle annular dark field [HAADF] scanning [S]TEM detector. Electron energy loss spectroscopy [EELS] analysis was carried out using a Philips CM200 FEGTEM operated at 197 keV and fitted with a Gatan GIF 200 imaging filter. All image, diffraction pattern processing and EELS spectrum processing was performed using Gatan Digital Micrograph software. Sections were prepared from areas on the femoral head displaying the most substantial tribolayer formation. These were identified as dark black regions located at the edge of the wear scars [see Fig. 1a]. Upon rinsing the samples, it was discovered that a substantial amount of white precipitate resided in the bearing interface. This was removed by rinsing and was stored in a desiccator for 24 h, by which time it had formed a brittle black flake. This was placed in distilled water, ground into a powder and pipetted onto a TEM holey support film on a Cu grid to enable microscopic inspection and chemical analysis.

To determine the composition of the tribolayer, EDX mapping was undertaken in the TEM at multiple locations. All EDX spectra and maps were processed using Aztec 2.0 and INCA 4.15 software. In addition, EELS was used to establish the degree of graphitisation within carbon rich regions of the tribolayer. Spectra were collected in diffraction mode with a collection semi-angle of approximately 1.7 mrad [to satisfy “magic angle” conditions] and a convergence angle of approximately 1 mrad [17].

3. Results

3.1. Transmission electron microscopy [TEM]

TEM images show that the tribolayer thickness varied across the sample, depending on the topography of the underlying surface. In regions where the surface was level

there was little variation in tribolayer thickness; however, in regions where the surface was rough the layer appeared to fill in the crevices [see Fig. 1b]. The range of thickness of the tribolayer observed was 200 nm-740 nm.

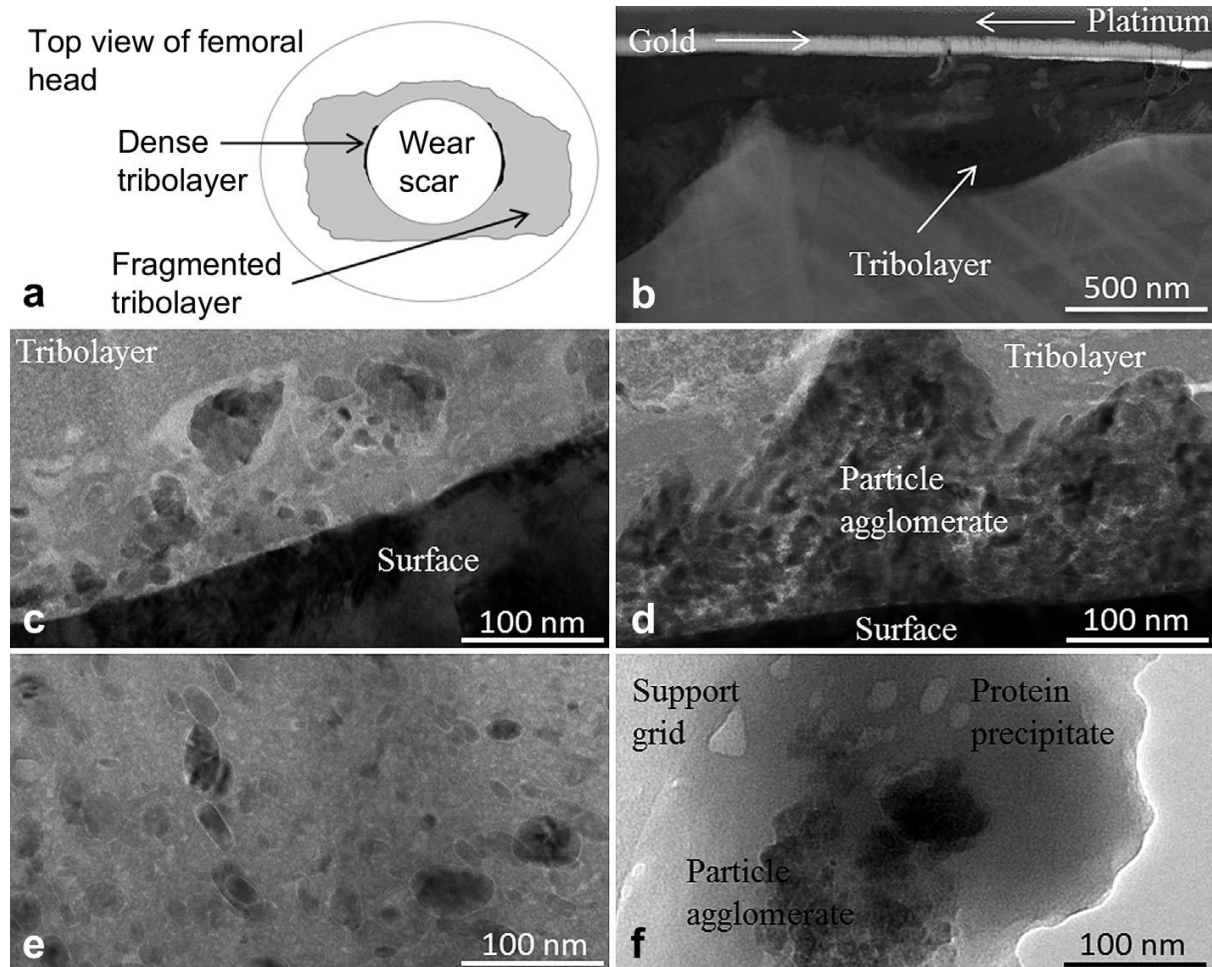


Fig. 1. a. Illustration of femoral head, showing tribolayer and wear scar. b. HAADF STEM image of bearing surface and tribolayer. c. Bright field TEM image of particles located at the surface/tribolayer interface. d. Bright field TEM image of agglomerated particles in tribolayer. e. Bright field TEM image of particles suspended in the tribolayer. f. Bright field TEM image of dehydrated protein precipitate containing agglomerated particles.

The tribolayer in each case was found to contain embedded particles, these were either: located at the surface/layer boundary [see Fig. 1c], agglomerated within the layer [see Fig. 1d] or independently suspended within it [see Fig. 1e]. Particles were typically smooth and oval shaped, however, some larger more jagged particles were identified at the surface/layer interface. The average length of oval particles was 24.2 nm with a range of 8.3 nm- 75.7 nm, whilst the average breadth was 14.9 nm with a range of 3.6 nm-34.4 nm, giving an average aspect ratio of 1.7. These results were obtained from the measurement of 130 particles, identified from bright field TEM images taken of the tribolayer.

TEM images of the protein precipitate, collected from the bearing interface, revealed that it also contained particle agglomerates. Agglomerates were observed to exceed

100 nm in length and breadth [see Fig. 1f]. The agglomeration of particles in these instances could be an artefact of the sample preparation. Dehydrating the precipitate and grinding it into a powder may cause agglomeration of particles contained within it.

3.2. Energy dispersive X-ray spectroscopy [EDX]

EDX mapping of the tribolayer revealed that it consisted of: carbon, calcium, cobalt, chromium, sulphur and oxygen. The particles embedded within the layer were comprised of cobalt and sulphur as shown in Fig. 2a and b; this was true for each of the three types of particle described earlier. When employing EDX analysis there is overlap of the 2.29 keV spectral peak of molybdenum and the 2.31 keV spectral peak of sulphur. Observation of the EDX spectrum from the tribofilm showed the 17.45 eV spectral peak associated with molybdenum was not present. This confirmed that particles were indeed rich in sulphur, not molybdenum.

It is possible to calculate standardless semi-quantification values from EDX spectra and maps. When this was applied to the particle agglomerates, it was found that their average elemental atomic composition was 59% cobalt and 41% sulphur. Particles at the surface/tribolayer interface [Fig. 1c] had an almost identical composition of 58% cobalt and 42% sulphur despite having a very different morphology. In regions of the tribolayer where particles were not observed, the average elemental composition by mass was: 63% oxygen, 10% chromium, 14% carbon, 6% cobalt, 5% phosphorus and 3% calcium. Compositions were calculated from an average of 5 spectra collected at different locations. The probe size used was approximately 50 nm.

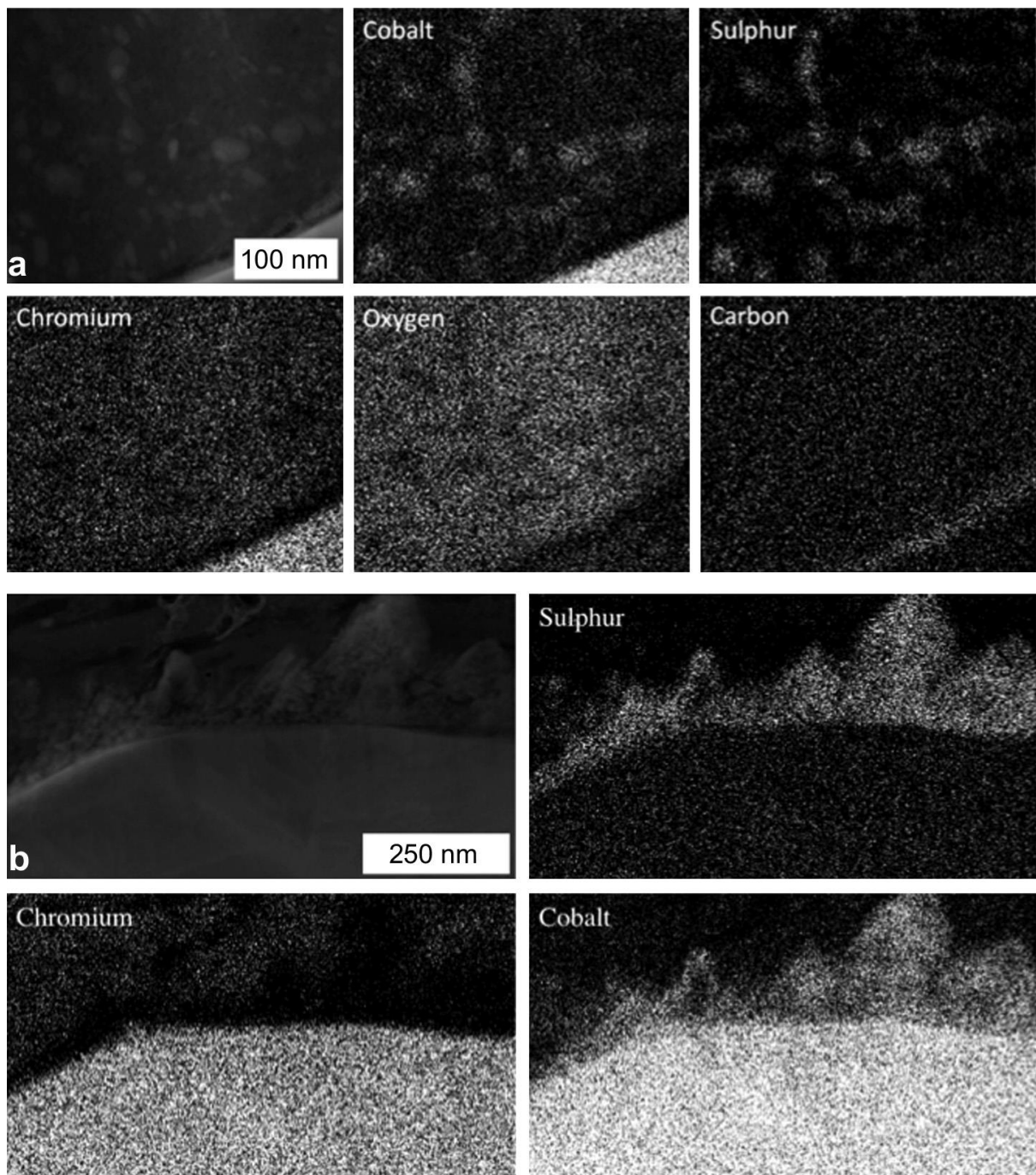


Fig. 2. a. HAADF STEM image and corresponding EDX map of particles suspended in tribolayer. b. TEM image and corresponding EDX map of particles agglomerated in tribolayer.

EDX spectra were taken from the base alloy at depths between 50 and 500 nm beneath the tribolayer. It was found that at all depths the composition of the alloy was within the specified composition given by ASTM standard F1537-08. This indicated that, a measurable amount of, preferential leaching of alloying elements had not taken place.

Spot EDX was also performed on the dehydrated protein precipitate. This revealed that it was predominantly comprised of carbon, oxygen and nitrogen. The

agglomerated particles within it contained chromium sulphur and cobalt in a ratio of 3.7; 1.4; 1 respectively.

3.3. Electron energy loss spectroscopy [EELS]

Core loss EELS spectra were obtained of the carbon K-edge from within the tribolayer. Fig. 3a shows a spectrum collected from within the tribolayer, alongside spectra obtained from amorphous carbon and highly ordered pyrolytic graphite [HOPG]. The spectrum obtained from the tribolayer has an appearance similar to that of amorphous carbon. It contains a sharp π^* peak close to 285 eV followed by a broad σ^* peak. Whereas, for HOPG the π^* peak was sharper and the σ^* peak and contained more features.

It is well known that electron beam damage can affect the sp^2/ sp^3 bonding ratio within carbon species [16,18-20]. To ensure that this was not taking place, a damage series was performed on a separate sample of the tribofilm. EELS spectra were taken at a point within the tribolayer periodically following exposure to the electron beam for 0,1,2,3,4,5 and 10 min; hence, the effect of electron fluence on EELS measurements was observed. The normalised periodic spectra obtained from the damage series are given in Fig. 3b. This shows that no discernable change in the EELS spectra was observed up to a total electron fluence of 1950 e/nm^2 [$t = 600 \text{ s}$].

Single spectra taken from different areas of the tribolayer were taken at lower total electron fluence, hence they were assumed to be free from significant beam damage.

Discussion

4.1. Effect of wear on contact mechanics

The location of the tribolayer as shown in Fig. 1a may be explained by the change in geometry of the head/cup interface following conformal changes brought about by wear. As the head and cup wear together the surfaces become more conformal within the wear scar. This is caused by a local increase in radius on the femoral head and a decrease in radius on the acetabular cup. This produces a very slight wedge on the border of the unworn surface and the wear scar.

The angle α is close to 90° since the change in radii is small relative to the initial radii, however, it is not negligible and increases as a function of the half-width of the wear scar. As wear progresses the radii tend to converge to a value midway between the two, and the effect of wear scar half width on wedge angle α can be calculated.

The pressure distribution exerted by a blunt wedge as shown in Fig. 4a is represented by Equation (1) when α is close to 90° [21].

$$p(x) = \frac{E^* \cot \alpha}{\pi \cosh^{-1} \left(\frac{\alpha}{x} \right)} \text{ and } P = \alpha E^* \cot \alpha \quad (1)$$

From Equation (1) and Fig. 4a, it can be seen then that under dry conditions the pressure rises to ∞ at $x = 0$. By modelling the edge of the wear scar as a blunt wedge it can be demonstrated that close to the edge of the wear scar there exists an area of increased pressure.

It is this predicted region of high pressure, which is where the thickest tribolayer formations occur. The scraping action of the blunt wedge, or the increased contact pressure it causes may contribute to the formation of the tribofilm at its location. As the wear scar increases in diameter the wedge becomes more defined and the contact pressure increases further.

4.2. Particle composition

Particles suspended within the tribolayer were on average just 24 nm in length and 15 nm in width, which are smaller than typical particle sizes produced in MoM bearings, during simulator testing [4-7]. In addition, the oval particles in the tribolayer appeared smoother than the oval particles previously imaged by Catelas et al. [4] or Bowsher et al. [7]. The environment within the tribolayer could be responsible for this difference. They may be smoothed due to repeated impacts with one another caused by high shear rates across the layer. This is a similar mechanism to the saltation process that leads to the size reduction and smoothing of suspended pebbles in rivers [22,23].

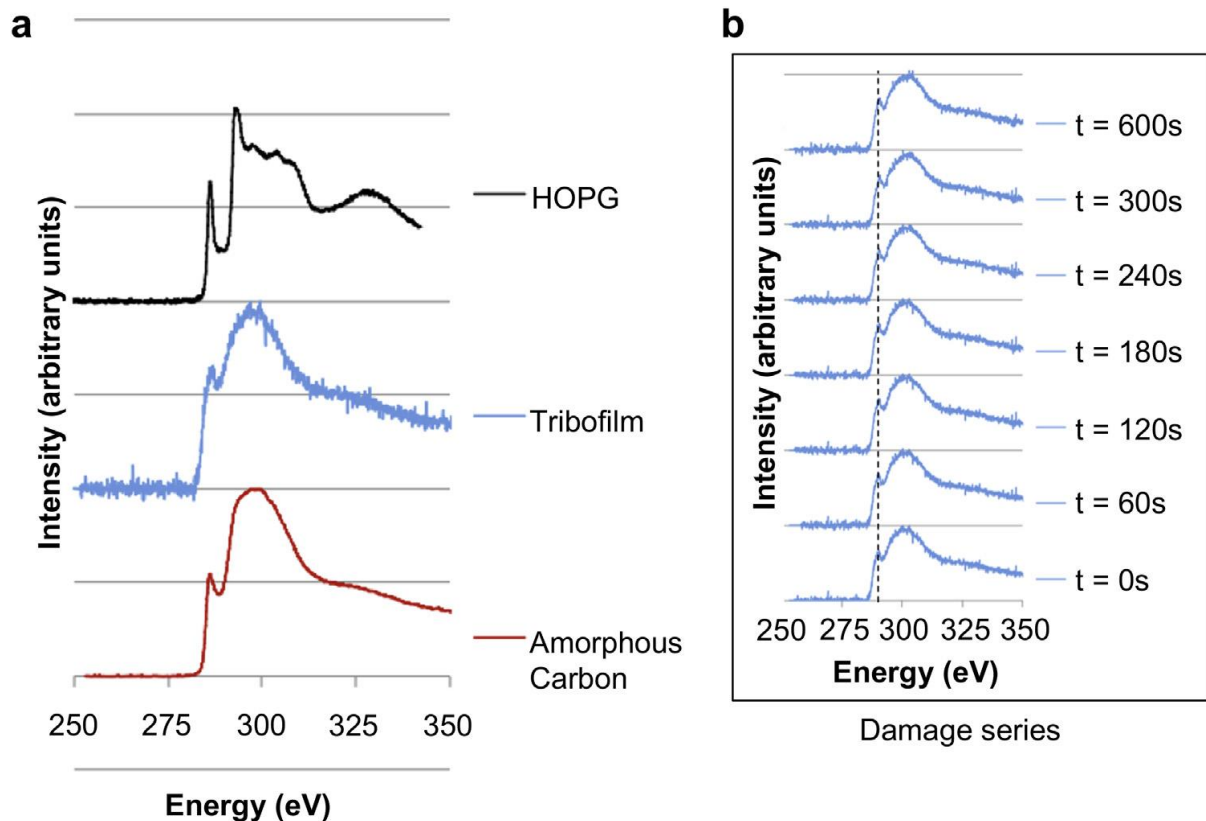


Fig. 3. a. Electron energy loss spectra, taken from the tribolayer compared to HOPG and amorphous carbon. b. EELS spectra taken after increasing electron fluence.

Particles that were observed close to the interface between the alloy surface and the tribolayer [Fig. 1c], appeared more jagged and larger than those suspended within the layer. These could be newly formed particles that had not yet been dispersed throughout the layer, and had not reduced in size through abrasion induced smoothing. This mechanism is partly supported by the presence of particle agglomerations. Agglomerations show that particles do translate within the layer and come into physical contact with one another.

EDX revealed that particles were comprised purely of cobalt [58-59% - atomic] and sulphur [41-42% - atomic]. No known sulphides of cobalt have a concentration of cobalt this great. This indicates that particles must also contain an amount of pure cobalt.

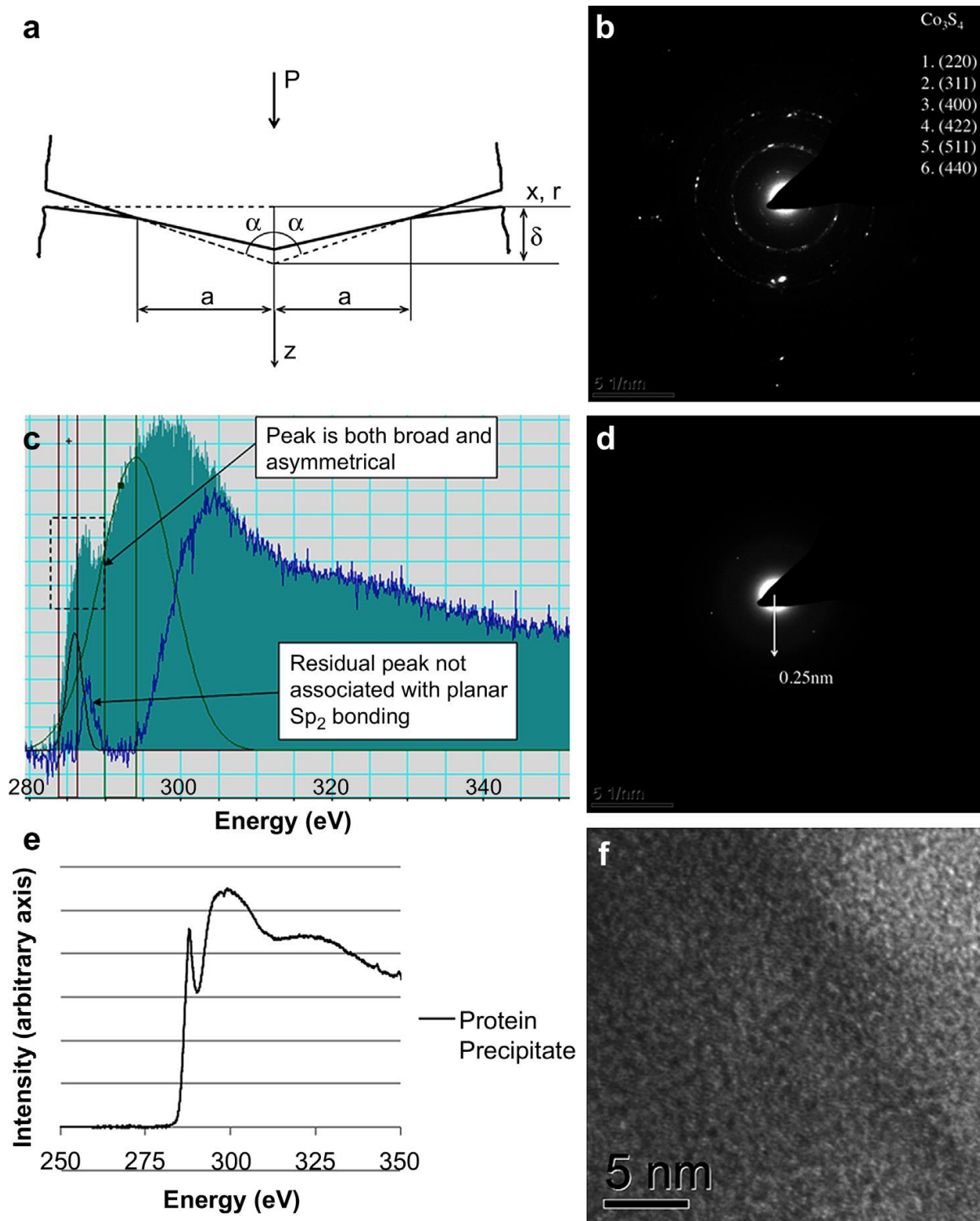


Fig. 4. a. Contact of a blunt wedge (21). b. Electron diffraction taken from agglomerated particles, indexed against cobalt sulphide (Co_3S_4). c. Fit used to estimate sp_2 bonding ratio in tribofilm. d. Electron diffraction pattern from tribolayer containing no embedded particles. e. EELS spectra of desiccated protein precipitate. f. TEM image of tribofilm.

Since the percentage composition of particles was irrespective of particle size, it is unfeasible that particles contain a cobalt core surrounded by a cobalt sulphide layer. Instead, it appears as if particles consist of a mixture of cobalt and cobalt sulphide. Electron diffraction patterns taken from the agglomerated particle were indexed

against cobalt sulphide [Co₃S₄] as shown in Fig. 4b. The composition of these particles differs from those typically found from both in vivo and in vitro studies, which seldom report cobalt in isolation from chromium due to its preferential dissolution from CoCr alloys.

The absence of chromium within the embedded particles may explain the high level of chromium within the tribolayer. In the base alloy, the ratio of cobalt to chromium was between 2.8 to 1 and 2 to 1, whereas the average ratio detected in the tribolayer was 1-1.4. Measurements of the composition of the base alloy just below the tribolayer indicated that no preferential leaching of alloying elements had taken place. This suggests that particulate debris was the primary source of cobalt and chromium within the tribofilm.

Furthermore, it appears that the concentration of cobalt within the embedded particles reduced the amount of freely available cobalt to distribute about the film, explaining the high ratio of chromium to cobalt within it. EDX indicated that preferential leaching of alloying elements did not take place in the bulk alloy beneath the tribolayer. This indicates that the presence of cobalt and chromium within the layer originates from both particles and oxidation of the topmost surface. The exact mechanism by which cobalt and chromium are separated from one another to leave cobalt rich particles embedded within a chromium rich tribolayer is still unclear.

4.3. Tribolayer

EDX confirmed that the tribolayer was organometallic in nature, and rich in carbon, which is consistent with previous findings [12].

From Fig. 1b it can be seen that the tribolayer exists as a smooth layer across the roughened metal surface. Its appearance demonstrated that it was smoothed over surface asperities, which is consistent with the theories that suggest that it may operate as a solid lubricant [12,13,16]. EELS C K-edge spectra taken from the tribolayer contained a prominent π^* pre-edge peak, similar to that measured in previous studies [16]. However, the C K-edge spectra obtained more closely resembled that of amorphous carbon [16] rather than that of crystalline graphite. Using the Gaussian fitting procedure presented by Zhang et al. [16,20] the fraction of planar sp² bonded carbon atoms [the [planar sp² bonded carbon]/[total carbon] ratio and hence the degree of graphitisation] was determined to be of the order of $\approx 65\%$. For comparison, the same technique was performed on an area of amorphous carbon TEM support film, which gave an sp² bonded carbon fraction of $\approx 73\%$.

This was a considerably lower value than that determined by Liao et al. [16] and this discrepancy may perhaps be attributed to the different fitting procedure used to determine the sp² bonded carbon fraction.

It is noticeable that the measured p- peak at the EELS C K-edge of the tribofilm was both asymmetric and also broad [relative to that observed in amorphous carbon or graphite]. It was concluded that this π^- peak was in fact made up of two distinct peaks [see Fig. 4c]. It is suggested that the lower energy loss peak [at ca. 285 eV]

may be associated with non-planar sp^2 bonded carbon and possibly also carbon [singly] bonded heteroatoms such as hydrogen, nitrogen and/or oxygen. This postulate is supported by both the amorphous appearance of the region at high magnification [i.e. there is substantial curvature in the carbon-carbon bonds] as well as the high percentage of oxygen found to be present in the film [63%] as determined by TEM-EDX analysis. In addition, there may be the presence of hydrogen [and hence C-H bonding], which is extremely difficult to detect. Note if we assume that the p- peak at the EELS C K-edge of the tribofilm is composed of just a single peak caused by planar sp^2 bonded carbon, the values for the degree of graphitisation calculated are much higher and may even exceed 100%. It is believed this finding provides support for our interpretation of the π peak as being comprised of two separate peaks.

In addition, electron diffraction patterns were obtained from regions of the layer deficient in particles, shown in Fig. 4d.

Diffraction patterns taken from the tribofilm appear similar to those reported by Wimmer et al. [16], however, the dominant spacing differs; d was measured to be approximately 0.25 nm as opposed to 0.34 nm. When TEM images were taken of the tribofilm, no evidence of ranged ordering was observed [Fig. 4f]. Suggesting that graphitisation had not taken place within the tribofilm.

4.4. Protein precipitate

Initially, the protein precipitate appeared milky in colour, but upon desiccating for 24 h it became black and solidified. EDX confirmed that the solid precipitate was rich in carbon and contained metallic particles. EELS spectra of the carbon k-edge of the layer indicated that it also displayed a prominent π^* pre-edge peak [Fig. 4e] and ca 74% planar sp^2 bonding.

It is clear that there are a number of similarities between the precipitated protein and the tribolayer. The comparable amount of sp^2 bonding, and sulphur containing metallic particles may indicate that the precipitation of proteins from the solution is a precursor to tribolayer formation. The tribofilm itself contained cobalt and chromium, whereas the precipitate only demonstrated cobalt and chromium within the entrapped particles. Particles may react with sulphur whilst trapped within precipitated proteins, but were only observed to lose their chromium content within the tribofilm.

Conclusions

The tribolayer that forms on the surface of MoM hip replacements under simulated gait was investigated using a TEM. It was revealed that the film was organometallic in nature and contained a number of embedded particles. Particles embedded within the film had a smaller and smoother morphology than those typically ejected from the bearing surface comprising entirely cobalt and sulphur. The film itself contained a large amount of carbon, although no evidence of graphitisation was seen from EELS or otherwise. Further understanding of the processes that lead to the formation of

tribolayers in MoM hip replacements may help to drive future material choices that can maximise their role as a solid lubricant within bearing surface.

Acknowledgements

The authors express their gratitude towards the Leeds Electron Microscopy and Spectroscopy Centre and particularly Professor Rik Brydson, for his support in the interpretation of EELS spectra.

References

- [1] Porter M., Borroff M., Gregg P., Howard P., MacGregor A., Tucker K, et al. The national joint registry for England and Wales 9th annual report 2012. http://www.njrcentre.org.uk/njrcentre/Portals/0/Documents/England/Reports/9th_annual_report/NJR%209th%20Annual%20Report%202012.pdf, [accessed 10.10.12].
- [2] Unsworth A. Recent developments in the tribology of artificial joints. *Tribol Int* 1995;28(7):485-95.
- [3] Dowson D. New joints for the millennium: wear control in total replacement hip joints. *Proc Inst Mech Eng Part H J Eng Med* 2001;215(4):335-58.
- [4] Catelas I, Bobynd JD, Medley JB, Krygier JJ, Zukor DJ, Huk OL. Size, shape, and composition of wear particles from metal-metal hip simulator testing: effects of alloy and number of loading cycles. *J Biomed Mater Res Part A* 2003;67(1): 312-27.
- [5] Tipper JL, Firkins PJ, Besong AA, Barbour PSM, Nevelos J, Stone MH, et al. Characterisation of wear debris from uhmwpe on zirconia ceramic, metal-onmetal and alumina ceramic-on-ceramic hip prostheses generated in a physiological anatomical hip joint simulator. *Wear* 2001;250(1-12):120-8.
- [6] Brown C, Williams S, Tipper J, Fisher J, Ingham E. Characterisation of wear particles produced by metal on metal and ceramic on metal hip prostheses under standard and microseparation simulation. *J Mater Sci Mater Med* 2007;18(5):819-27.
- [7] Bowsher J, Hussain A, Williams P, Shelton J. Metal-on-metal hip simulator study of increased wear particle surface area due to 'severe' patient activity. *Proc Inst Mech Eng Part H J Eng Med* 2006;220(2):279-87.
- [8] Case C, Langkamer V, James C, Palmer M, Kemp A, Heap P, et al. Widespread dissemination of metal debris from implants. *J Bone Jt Surg Br Vol* 1994;76-B(5):701-12.
- [9] Hodgson AW, Mischler S, Von Rechenberg B, Virtanen S. An analysis of the in vivo deterioration of co-cr-mo implants through wear and corrosion. *Proc Inst Mech Eng Part H J Eng Med* 2007;221(H3):291-303.
- [10] Savarino L, Granchi D, Ciapetti G, Cenni E, Nardi Pantoli A, Rotini R, et al. Ion release in patients with metal-on-metal hip bearings in total joint replacement: a comparison with metal-on-polyethylene bearings. *J Biomed Mater Res* 2002;63(5):467-74.
- [11] Savarino L, Granchi D, Ciapetti G, Cenni E, Greco M, Rotini R, et al. Ion release in stable hip arthroplasties using metal-on-metal articulating surfaces: a comparison between short- and medium-term results. *J Biomed Mater Res Part A* 2003;66A(3):450-6.

- [12] Wimmer MA, Sprecher C, Hauert R, Täger G, Fischer A. Tribochemical reaction on metal-on-metal hip joint bearings: a comparison between in-vitro and invivo results. *Wear* 2003;255(7-12):1007-14.
- [13] Wimmer MA, Fischer A, Büscher R, Pourzal R, Sprecher C, Hauert R, et al. Wear mechanisms in metal-on-metal bearings: the importance of tribochemical reaction layers. *J Orthop Res* 2009;28(4):436-43.
- [14] Yan Y, Neville A, Dowson D. Biotribocorrosion of cocrmo orthopaedic implant materials assessing the formation and effect of the biofilm. *Tribol Int* 2007;40(10-12):1492-9.
- [15] Yan Y, Neville A, Dowson D, Williams S, Fisher J. Tribofilm formation in biotribocorrosion e does it regulate ion release in metal-on-metal artificial hip joints? *Proc Inst Mech Eng Part J J Eng Tribol* 2010;224(9):997-1006.
- [16] Liao Y, Pourzal R, Wimmer MA, Jacobs JJ, Fischer A, Marks LD. Graphitic tribological layers in metal-on-metal hip replacements. *Science* 2011;334(6063):1687-90.
- [17] Daniels H, Brown A, Scott A, Nichells T, Rand B, Brydson R. Experimental and theoretical evidence for the magic angle in transmission electron energy loss spectroscopy. *Ultramicroscopy* 2003;96:523-34.
- [18] McCulloch DG, McKenzie DR, Prawer S, Merchant AR, Gerstner EG, Kalish R. Ion beam modification of tetrahedral amorphous carbon: the effect of irradiation temperature. *Diam Relat Mater* 1997;6(11):1622-8.
- [19] Davis CA, Knowles KM, Amaratunga GAJ. Cross-sectional structure of tetrahedral amorphous carbon thin films. *Surf Coat Technol* 1995;76:316-21.
- [20] Zhang ZI, Brydson R, Aslam Z, Reddy S, Brown A, Westwood A, et al. Investigating the structure of non-graphitising carbons using electron energy loss spectroscopy in the transmission electron microscope. *Carbon* 2011;49(15): 5049-63.
- [21] Johnson KL. *Contact mechanics*. Cambridge University Press; 1985.
- [22] Pittman ED, Ovenshine AT. Pebble morphology in the Merced river [California]. *Sediment Geol* 1968;2(2):125-40.
- [23] Schumm SA, Stevens MA. Abrasion in place: a mechanism for rounding and size reduction of coarse sediments in rivers. *Geology* 1973;1(1):37-40.